A Rule-Based Fire Spread Model for Simulating Prescribed Burns

Gary L. Achtemeier•
USDA Forest Service, Athens, GA

1. INTRODUCTION

Rabbit Rules (RR) was first introduced as an alternative method for calculating fire spread in 2003 (Achtemeier, 2003) [RR2003]. A rabbit is an autonomous agent (Flakes, 2000) that represents elements of fire. By definition, an agent is a substitute for the original, a proxy that performs a function similar to the function performed by the original. RR2003 was presented as a kind of novelty, a proof-of-concept experiment – a demonstration that the "agent model" concept possessed sufficient explanatory power to account for many of the patterns associated with fire spread.

Most models created to predict fire spread fall into one of two classes, empirical models and physical models. For empirical models (Finney, 1998), fire spread is measured under controlled conditions and a statistical relationship found between fire spread and each variable tested (Rothermal, 1972). The model typically is represented in two dimensions through predetermined geometry, for example, overlapping ellipses (Alexander, 1985). Empirical models have skill at low to moderate winds. However, at higher wind speeds and under conditions that produce erratic fire behavior, statistical/empirical methods are less skillful because the equations were not derived for such conditions.

Physical models describe fire spread as heat transfer between burning and unburned fuel through coupled differential equations (Clark, et al, 1996; Linn, 1997; Linn and Harlow, 1998). Physical models can explain mathematically how combustion processes in heterogeneous fuels under variable atmospheric condition translate to fire behavior and thence to fire spread. In addition, physical models explain nonlinear processes such as complex fire-atmosphere feedbacks that can account for extreme fire behavior. Physical models can generate complex patterns of fire spread over complex terrain in heterogeneous fuels.

The agent model (Rabbit Rules) describes fire spread by simulating the fire through a set of rules and simple equations cast as computer programs solved recursively (Wolfram, 2002). Fire spreads in three ways: 1) Radiation from burning fuels heats adjacent fuels to ignition. 2) Convective currents carry burning gases across adjacent fuels causing ignition. 3) Burning embers fall into adjacent fuels causing ignition (local spotting). Rabbit Rules is based on the third mechanism of fire spread.

Rules governing RR were summarized in RR2003. This paper summarizes the impact of the coupled fire–atmosphere interaction rule A1 on fire/plume-induced local winds. Because the simple equations that drive RR are weighted by coefficients, it is necessary to validate RR with case studies. RR was run for the 23 February 2006 FireFlux experiment (Clements, et al., 2007). Results for Case 4 are summarized below.

2 . MATERIALS & METHODS

Details of the FireFlux experiment may be found in Clements et al. (2007). Data from FireFlux used for this study include temperature and 2m wind measurements at the main and south towers. Observations of fire spread, time and place of ignition, and dimensions of the area burned were used to initialize RR.

Microsoft Paint provides the graphical user interface for RR. The graphic provides two-way communication between the user and the model. RR interrogates each pixel for information regarding fire starts (light yellow), existing fire (orange), declining fire (red), fuel type and fuel characteristics (shades of green), fire breaks (non-green colors), and burned areas (black). At any time during execution, the user can stop RR to add fire, change fuel conditions, and modify fire breaks.

Figure 1 shows the MS Paint approximation to the FireFlux experimental area. The area burned was 450 x 750 m with a rectangular area notched from the lower right hand side. The fuel (shaded green) was a homogeneous distribution of natural prairie grass approximately 2 m deep. Locations of the main and south towers where time series of the velocity components of the wind were collected as part of FireFlux and outputted from RR are identified by the blue squares.

Ignition began at 1243:40 CST at the small yellow line identified by the arrow in Figure 1. Burn crews with drip torches walked in both directions to complete the burn line across the north end of the experimental area. This time-dependent pattern of ignition was approximated in RR by stopping the

• *Corresponding author address:* Gary L. Achtemeier, Forest Sciences Laboratory, 320 Green Street, Athens, GA 30602; e-mail: gachtemeier@fs.fed.us.

model every 30 sec and adding a short yellow line segment to the existing burning area until the burn line was completed.

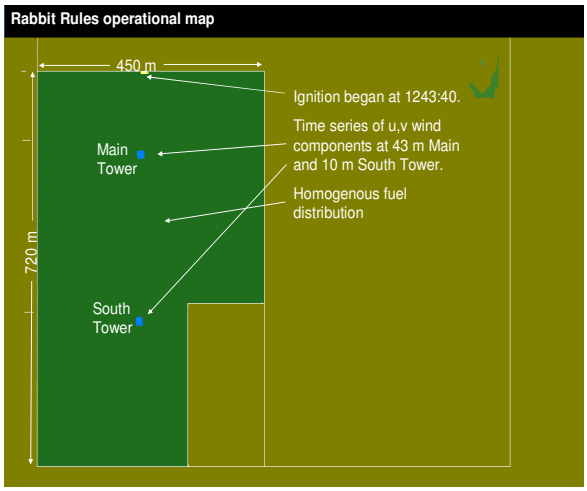

Figure 1. RR operational approximation to the FireFlux experimental area constructed via MS Paint.

The coupled fire–atmosphere interaction rule A1 for RR posits that each rabbit produces a plume of heated air that drifts downwind from the rabbit location. This plume of warm air creates a tiny hydrostatically-induced low pressure area at the ground. The rationale for rule A1 is that a smoke plume carries heated air within a layer of depth dz above the ground (Figure 2). A small low pressure area exists beneath the plume. The magnitude of the low pressure area is determined by the depth of the plume and the increase of plume temperature above the temperature of ambient air.

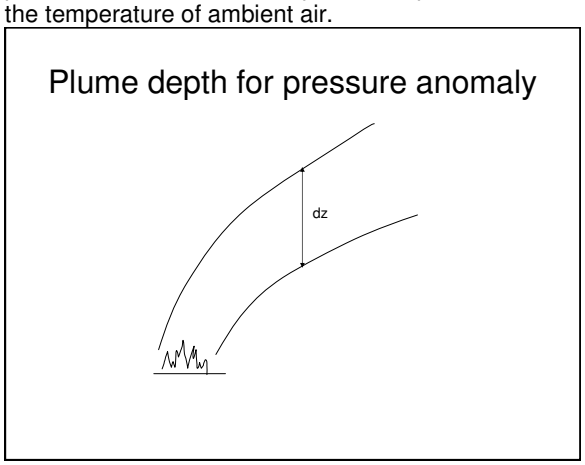

Figure 2. Schematic of heated plume of depth dz.

Figure 3 shows the temperature anomaly required to produce a given pressure anomaly for a specified plume thickness. For example, if a plume is 100m deep, then a temperature anomaly of 8.0C will produce a pressure anomaly of -0.3 mb.

In RR, the downwind shape and relative magnitude of the low are defined by a set of 10 coefficients. The magnitude of the low was set to -0.0003 mb per rabbit for Case 4. When summed over a large number of rabbits, the low pressure area can become large enough to impact winds locally. For Case 4, the "maximum" pressure anomaly was -0.3 mb.

Temperature anomaly required to produce a given pressure anomaly for given plume thickness

dz (m)	-0.1 mb	-0.2 mb	-0.3 mb	-0.4 mb	-0.5 mb	-1.0 mb
20	13.5	28.3	44.5	62.4	82.3	226.9
40	6.6	13.5	20.7	28.3	36.2	82.3
60	4.4	8.9	13.5	18.3	23.2	50.3
80	3.3	6.6	10.0	13.5	17.1	36.2
100	2.6	5.3	8.0	10.7	13.5	28.3
120	2.2	4.4	6.6	8.9	11.2	23.2
140	1.9	3.7	5.6	7.6	9.5	19.7
160	1.6	3.3	4.9	6.6	8.3	17.1
180	1.4	2.9	4.4	5.9	7.4	15.1
200	1.3	2.6	3.9	5.3	6.6	13.5

Figure 3. Temperature and pressure anomalies as functions of the depth of smoke plumes.

Rabbit Rules was embedded within the wind model PB-Piedmont (Achtemeier, 2005). Maximum resolution within PB-Piedmont determined by the resolution of the USGS national elevation data set is 30m. Therefore no effort was made to model circulations on the scale of the fire. The effort was directed at modeling plume-driven winds at a scale one order of magnitude greater and resolvable by the model. RR was initialized with winds of 020 degrees at 4 m sec^{-1}. "Upper" winds needed for calculating downward horizontal momentum transport were set at 020 degrees at 6 m sec^{-1}. Base fire spread rate (0.23 m sec^{-1}) for grass, fuel height (2 m), and rabbit weight (0.4 kg) were set to yield the observed spread rate of 1.3 m sec^{-1}. The average fire residence time at any rabbit location was set at 20 sec.

3 . RESULTS

Figure 4 shows the RR simulated fire and associated wind field at 1244:40 CST, just one minute after ignition. Wind speeds and directions are shown on the 30 m PB-Piedmont grid. The long barb equals 5 m sec^{-1} and the short barb equals 2.5 m sec^{-1}. Contours of pressure are given in tenths of mb. The "lobed" appearance of the fire line is the outcome of stopping RR every 30 sec to complete the ignition line segment by segment.

A -0.3 mb pressure anomaly is found at the head of the fire. The pressure field tails off along a single lobe identified by the dashed line. The pressure field turns the winds to converge toward the dashed line. The asymmetry is the outcome of ambient winds blowing 20 degrees off from the axis of the burn.

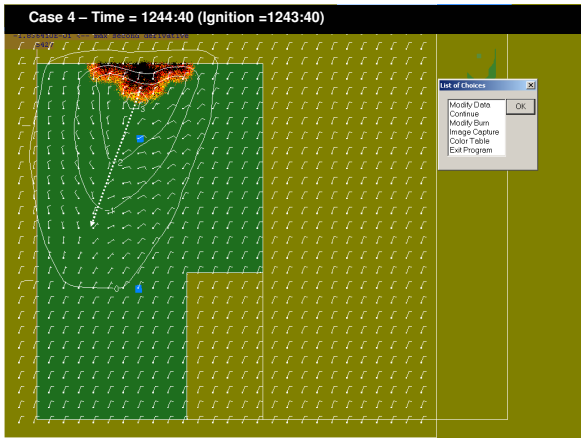

Figure 4. Map of fire spread one minute after ignition.

As the fire line lengthened, the pressure lobe in Figure 4 separated into two lobes oriented roughly with the prevailing wind (solid lines in Figure 5). The asymmetry in the wind field increased and there appeared two confluence zones (dashed lines).

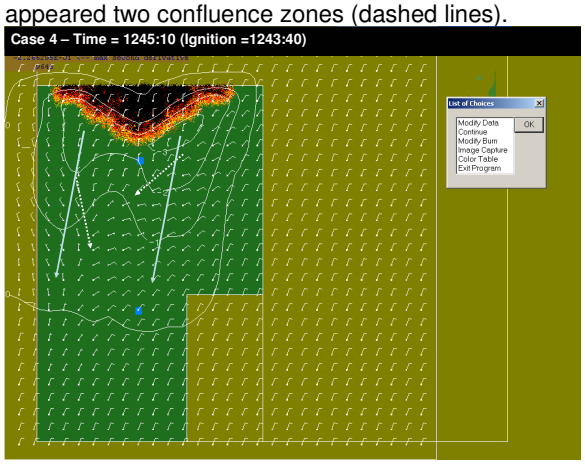

Figure 5. Same as Figure 4 except for 1.5 min after ignition.

Figure 6 shows time series of the U-component of the wind and the temperature at 2 m at the main tower from FireFlux. The U-component is defined as the wind blowing down the area of the burn along an axis normal to the fire line and of sign positive in the direction of fire spread. The red rectangle locates from the temperature series the likely period that the fire passed the tower. The green line represents the time series of the U-component of the wind as simulated by RR.

RR captures a small decline in the wind speed just before 1246 CST followed by a rise to 8 m sec^{-1} just before the fire. The magnitude is correct (RR did not simulate the brief wind shift – negative U) but is shifted out of phase. Thus RR simulated the event too soon by approximately 15 sec. An explanation for the discrepancy holds that the fire was just getting underway and the plume was not yet fully organized. Figure 7 shows relative emissions production simulated by RR for FireFlux. The fire line passed the main tower just as the fire reached maximum coverage. Thus it could be argued that the plume was still developing. RR equations for plume-induced low pressure are based on an assumption of a mature plume and would have placed the impacts of the plume too far downwind. Thus the low pressure anomaly could have impacted the location of the main tower too soon.

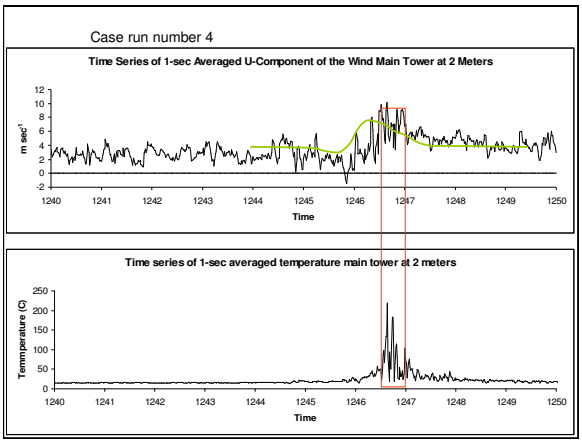

Figure 6. Time series of the U-component of the wind and temperature at 2 m at the main tower.

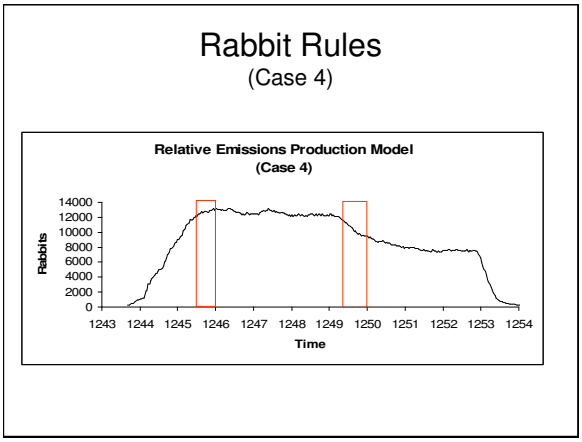

Figure 7. Relative emissions for FireFlux as simulated by Rabbit Rules.

The plume was fully developed by the time the fire had spread to the south tower. Figure 8 shows the fire line and associated asymmetric wind and pressure fields. The asymmetry in the fire line is the outcome of the interaction of the fire with the prevailing winds which blew with a V-component from the east (negative). The response of the RR pressure field to the distribution of fire within the ambient wind was to create conditions for strong east wind to blow across the entire field to the convergence zone located along the left (west) side of the field.

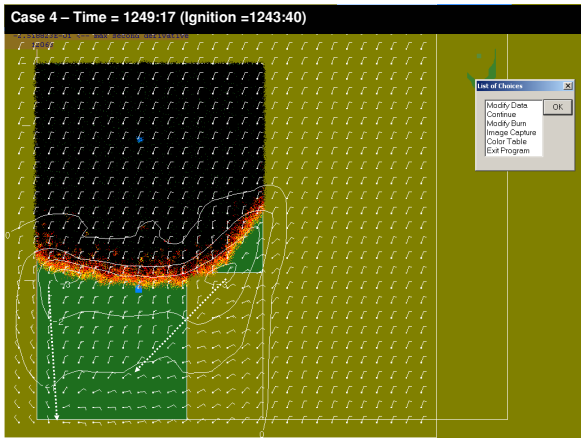

Figure 8. Map of fire spread at 1249:17 CST.

Figure 9 shows the time series of the U-component of the wind and temperature at 2 m at the south tower during FireFlux. Beginning at 1246 CST, wind speed decreased from approximately 4 m sec^{-1} to -1.8 m sec^{-1} (wind shift to blow from the south toward the fire) at 1247:35 CST. Then U increased to 8 m sec^{-1} with gusts to 10 m sec^{-1} by 1250 CST. A sharp drop in the wind speed at 1250:05 CST was linked to fire-driven circulation (Clements, et al., 2007). Wind speeds peaked near 12 m sec^{-1} at 1250:30 CST at the beginning of the fire than tapered off to near 4 m sec^{-1} by 1253 CST.

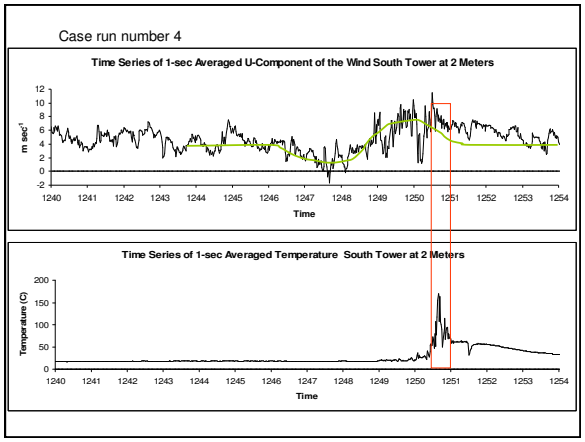

Figure 9. Time series of the U-component of the wind and temperature at 2 m at the south tower.

The U-component wind speed simulated by RR is shown by the solid green line referenced to the time of fire passage at the tower given for FireFlux. The plume-generated pressure field slowed winds beginning at 1246 CST from 4 m sec^{-1} to a minimum of approximately 1 m sec^{-1} near 1247:45 CST. Then winds increased to near 8 m sec^{-1} shortly before 1250 CST. This trace closely matched the general pattern of the U-component time series. After 1250 CST, the RR solution fell out of phase with the FireFlux time series of U. This period included the fire induced circulation (RR does not simulate this) and the tail-off of wind speed following the fire (RR winds had decreased to ambient speeds by 1251:30 CST.

4 . DISCUSSION

Since the coupled fire-atmosphere interaction rule generates its own wind field, the purpose of this study is to compare RR winds with observed winds for FireFlux at both the main and south towers. Two questions are implied:

1) Are the FireFlux winds impacted by plume scale forcing?
2) Do the RR-simulated winds explain plume scale features observed in the FireFlux winds?

The answer to both questions appears to be “Yes”.

The coupled fire–atmosphere interaction rule A1 for RR posits that each rabbit produces a plume of heated air that drifts downwind from the rabbit location. The sum of the low pressure areas for all rabbits can create a pressure field of sufficient strength to modify winds locally. The winds generated by rule A1 are summarized by the following schematics.

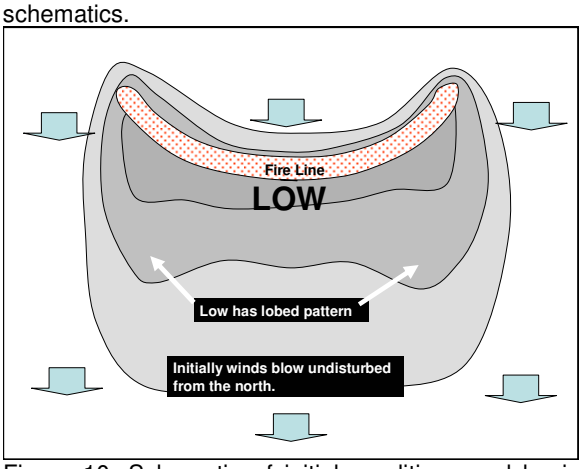

Figure 10. Schematic of initial conditions and basic pressure field for RR rule A1.

The fire line is represented by the red-dotted rectangle in Figure 10. Heated air departing the fire creates a hydrostatic low pressure area just downwind from the fire. This low expands downwind and weakens as the plume drifts downwind and cools. The direction of drift is the ground-level wind direction at the location of each rabbit (fire element). Near the ends of the fire line, the pressure gradient turns the wind to blow more towards the low pressure area. This causes the incremental low pressure patterns to overlap reinforcing the low locally and creating the lobed pattern shown in the figure.

The impact of the pressure field on the local winds is shown schematically in Figure 11. Air approaching the fire is accelerated by the strong pressure gradient across the fire to blow through the fire at high velocity. The pressure gradient extending downwind from the flanks of the fire line turns the

winds to blow inward toward the low pressure area. Outbound air is slowed by the pressure field.

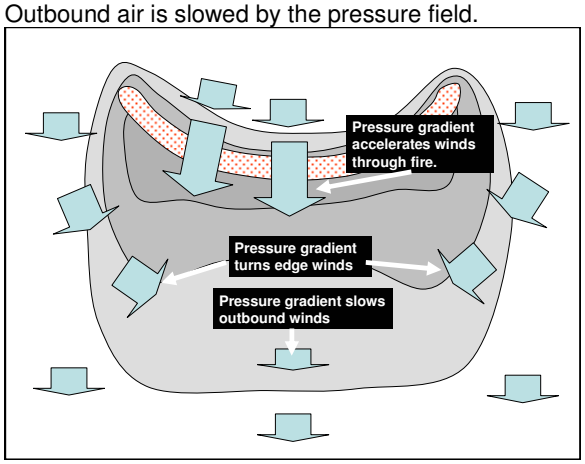

Figure 11. Schematic showing the impact of the plume-induced pressure field on the local winds.

Figure 12 shows the winds at a later time. Air accelerated through the fire slows in the reversed pressure gradient. Winds turned along the flanks of the fire converge toward a centerline ahead of the fire. Winds along the centerline weaken, stall, or reverse direction depending on the relative magnitudes of the plume-induced low pressure area and the ambient wind speeds.

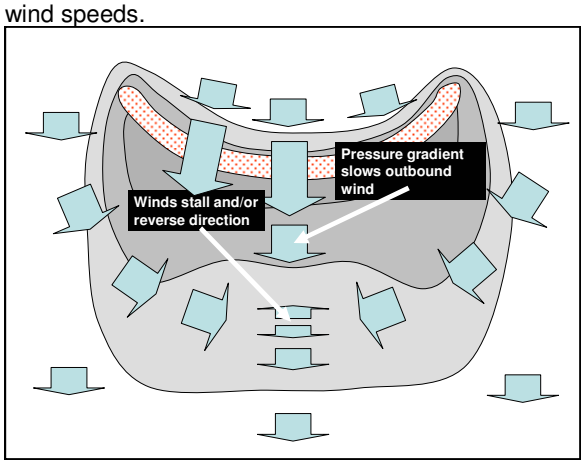

Figure 12. Same as for Figure 11 except for a later time.

The outcome is a convergence area shown in Figure 13. Air accelerated through the fire pushes ahead of the fire to collide with air turning ahead of the fire from the flanks. Given that air passing through the fire carries smoke, the convergence zone may mark the boundary of liftoff for the underside of the smoke plume.

The schematic RR wind fields may be over-simplified because they do not include plume scale turbulent mixing to the ground downwind from the fire. Figure 14 shows time series for the V-component of the wind and temperature at 2 m at the south tower. The green line shows RR winds referenced to the time of fire passage at the tower given for FireFlux. The RR solution follows the observations from 1246-1247 CST as the easterly winds increased from -2 m sec^{-1} to -4 m sec^{-1}. Then the solution departs from observations as the RR easterly wind speed increase to -6 m sec^{-1}. This is when the U-component reached its minimum. Thus, RR solutions in Figure 8 showed that winds ahead of the convergence zone were blowing directly from the east toward the confluence zone (dashed lines) running along the west boundaries of the burn area.

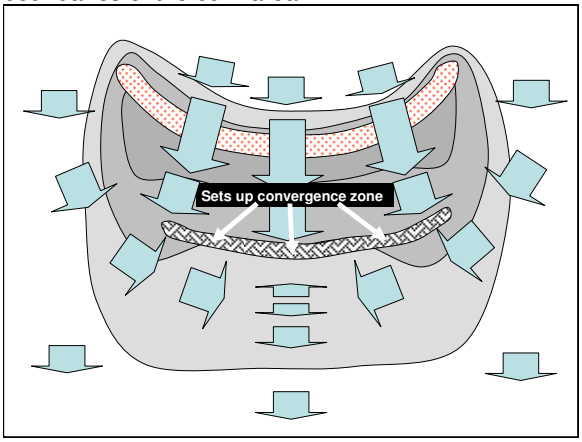

Figure 13. Schematic showing development of a convergence zone where winds accelerated through the fire encounter winds accelerated ahead of the fire from the flanks.

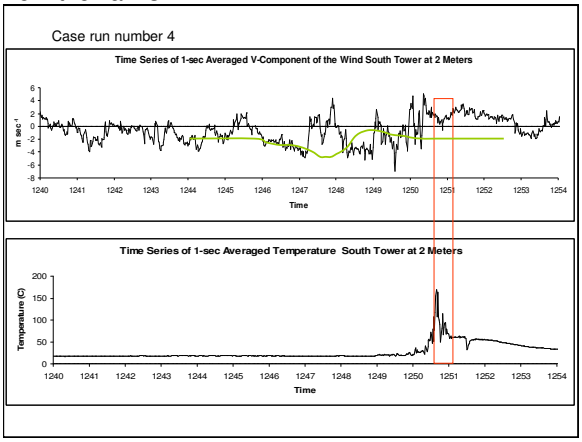

Figure 14. Time series of the V-component of the wind and temperature at 2 m at the south tower.

Meanwhile, observations show an abrupt shift in the V-component shortly after 1247 CST from -4 m sec^{-1} to +1 m sec^{-1} giving the impression that the wind had stalled according to Figure 12. Furthermore, the persistence of the shift added to the impression that the convergence zone in Figure 13 had passed the south tower.

The RR U-component increased after 1248 CST, while the V-component went to near zero and remained near ambient during the passage of the fire meaning the convergence zone had passed the south tower in the RR simulation. The observed wind, however, abruptly shifted to blow from the east at 1248:10 and remained from the east at 4 m sec^{-1} until 1249 CST. After 1249 CST, the V-component oscillated widely between 4 m sec^{-1} and -7 m sec^{-1}

until the passage of the fire when the V-component shifted to blow from the west.

Considering the average fire spread rate of 1.3 m sec^{-1}, the time series for the V-component can be converted to a spatial dimension with the fire at the origin and the V-component record extending downwind (measured negative in time). In this case, the V-component record shows short wavelength high amplitude turbulence (from 1250:30 to 1249) extending immediately downwind from the fire. At greater distance, the amplitude has decreased and the wavelength increased as should be expected as turbulent eddies within the plume cascade upwards to longer wavelengths. By 1248:10 – 1247:10 CST, (260-325 m from the fire) eddy size is 65m.

In summary, the Rabbit Rules coupled fire-atmosphere interaction rule A1 generates bulk wind fields that bear resemblance to winds observed during the 23 February 2006 FireFlux experiment. RR does not simulate strong turbulence observed in the V-component of the wind.

5. REFERENCES

Achtemeier, G.L., 2003: "Rabbit Rules" – An application of Stephen Wolfram's "new kind of science" to fire spread modeling. Fifth Symp. Fire and Forest Meteor., Orlando, FL, Amer. Meteor. Soc.

Achtemeier, G.L., 2005: Planned Burn – Piedmont. A local operational numerical meteorological model for tracking smoke on the ground at night: Model development and sensitivity tests. Int. J. Wildland Fire, 14, 85-98.

Alexander, M. E., 1985: Estimating length to breadth ratio of elliptical forest fire patterns. Proceedings of the Eighth Conference on Fire and Forest Meteorology. Society of American Foresters, p. 287-304.

Clark, T.L., M. A. Jenkins, J. Coen, and D. Packham, 1996: A coupled atmospheric-fire model: convective Froude number and dynamic fingering. Intl. Journal of Wildland Fire, 6: 177-190.

Clements, C.B., S. Zhong, S. Goodrick, J. Li, B. E. Potter, X. Bian, W. E. Heilman, J. J. Charney, R. Perna, M. Jang, D. Lee, M. Patel, S. Street, and G. Aumann, 2007: Observing the dynamics of wildland grass fires: FireFlux – a field validation experiment. (Accepted for publication in Bull. Amer. Meteor. Soc.)

Finney, M. A., 1998: FARSITE: Fire Area Simulator – model development and evaluation. USDA Forest Service Research Paper RMRS-RP-4, Rocky Mountain Research Station, Ft. Collins, CO, 47 pp.

Flakes, G. W. ,2000, The Computational Beauty of Nature: Computer Explorations of Fractals, Chaos, Complex Systems, and Adaptation, MIT Press. 514 pp.

Linn, R. R., 1977: Transport Model for Prediction of Wildfire Behavior. Los Alamos National Laboratory Scientific Report: LA13334-T.

Linn, R. R., and F. H. Harlow, FIRTEC: A transport description of wildfire behavior. 2nd Symposium on Forest and Fire Meteorology, American Meterological Society 78th Annual Meeting, Phoenix, AZ, 11-16.

Rothermal, R. C., 1972: A mathematical model for predicting fire spread in wildland fuels. USDA Forest Service Research Paper INT-115, Ogden, UT, 40 pp.

Wolfram, S., 2002: A New Kind of Science. Wofram Media, Inc., 1197 pp.